



## Original Article

# The Effect of Measurement Depth and Technical Considerations in Performing Liver Attenuation Imaging



Colby Adamson<sup>1</sup>, Jourdain Dong<sup>1</sup>, Lauren D. Hagenstein<sup>1</sup>, Joseph Jenkins<sup>1</sup>, Mark Lee<sup>2</sup> and Jing Gao<sup>1,2\*</sup>

<sup>1</sup>Rocky Vista University-Southern Utah, Ivins, UT, USA; <sup>2</sup>Rocky Vista University-Montana College of Osteopathic Medicine, Billings, MT, USA

Received: July 26, 2023 | Revised: November 08, 2023 | Accepted: December 20, 2023 | Published online: March 07, 2024

## Abstract

**Background and objectives:** Clinical unmet need in managing nonalcoholic fatty liver disease (NAFLD), a common liver disorder affecting 25–30% of American adults is to develop noninvasive and robust biomarkers.

**Methods:** We re-measured liver AC by placing a region of interest (ROI, 3 cm tall and 3 cm wide) at 4.5 cm, 6 cm, and 7.5 cm from the skin and a large ROI (6.0 cm tall and 7.3 cm wide) on pre-recorded ATI images from 117 participants screened for NAFLD. The difference in AC value at variable ROI depths was tested using one-way ANOVA (analysis of variance). Diagnostic performances of AC at variable depths in determining hepatic steatosis were examined by area under receiver operating characteristic curve (AUC) using MRI-proton density fat fraction (MRI-PDFF) as reference and were compared using paired-sample Z-test.

**Results:** Based on MRI-PDFF, 117 livers were divided to 27 normal livers (MRI-PDFF < 5%) or 90 steatotic livers (MRI-PDFF ≥ 5%). Differences in AUC and AC value at variable depths and size were statistically significant ( $p < 0.01$ ). The best performance for determining hepatic steatosis was the AC measured at 6 cm from the skin (AUC = 0.92). Sources of errors in performing ATI included reverberation, blank color region, and acoustic shadowing within the measurement ROI.

**Conclusions:** ROI depth significantly influences liver AC estimation. The best ROI depth to measure liver AC in patients with BMI ≥ 30 may be at a depth of 6 cm from the skin. Technical considerations should be taken in performing liver ATI.

## Introduction

The prevalence of nonalcoholic fatty liver disease (NAFLD) has seen a significant increase worldwide, with a 10% increase in a recent 5-year period.<sup>1</sup> NAFLD is now estimated to affect 25% of the general population, making it the most common chronic liver disorder in the world.<sup>2</sup> Moreover, there have been strong correlations between NAFLD and other metabolic syndromes such as diabetes mellitus

and obesity, cardiovascular disease, and chronic kidney disease reported.<sup>3,4</sup> Therefore, NAFLD is an ever-increasing healthcare concern in which early detection can result in better clinical outcomes.

Hepatic steatosis, defined as an accumulation of lipids within the liver parenchyma (>5%), can cause liver tissue injury. This damage begins with inflammation that results in liver scarring, which ultimately develops fibrosis in the liver. If left untreated, progression of fibrosis can lead to cirrhosis, which significantly increases the risk for developing liver failure and hepatocellular carcinoma.<sup>5</sup> Early stages of NAFLD are reversible and can be managed with lifestyle changes and medications, however, once progression is made to later stages, there are no approved treatments other than liver transplantation.<sup>6</sup> The current gold standard in the diagnosis of NAFLD is liver biopsy, which is highly efficacious for diagnosis throughout all stages of NAFLD, specifically in determining nonalcoholic steatohepatitis (NASH).<sup>7</sup> The liver biopsy, as with any invasive procedure, has the associated risks of pain, infection, bleeding, and unintended comorbidities that are significant; in addition to variation in tissue sampling and interpretation.<sup>8</sup>

Alternatively, there are non-invasive imaging modalities available for assessing NAFLD including computed tomography (CT), magnetic resonance imaging (MRI), serologic testing, and ultrasound. CT has shown to be an effective measure in assessing more advanced liv-

**Keywords:** Attenuation coefficient; Liver; Magnetic resonance imaging-proton density fat fraction; Nonalcoholic fatty liver disease; Ultrasound.

**Abbreviations:** AC, attenuation coefficient; ANOVA, one-way analysis of variance; ATI, ultrasound attenuation imaging; AUC, area under receiver operating characteristic curve; CI, Confidence Interval; MRI, magnetic resonance imaging; MRI-PDFF, magnetic resonance imaging-based proton density fat fraction; NAFLD, nonalcoholic fatty liver disease; NASH, nonalcoholic steatohepatitis; ROC, receiver operating characteristic; ROI, region of interest.

\*Correspondence to: Jing Gao, Ultrasound Research and Education, Rocky Vista University, Montana College of Osteopathic Medicine, 4130 Rocky Vista Way, Billings, MT 59106, USA. ORCID: <https://orcid.org/0000-0001-5993-042X>. Tel: +1-406-901-2726, E-mail: [jgao@rvu.edu](mailto:jgao@rvu.edu)

**How to cite this article:** Adamson C, Dong J, Hagenstein LD, Jenkins J, Lee M, Gao J. The Effect of Measurement Depth and Technical Considerations in Performing Liver Attenuation Imaging. *J Transl Gastroenterol* 2024;2(1):1–8. doi: 10.14218/JTG.2023.00047.

er disease but is insufficient in detecting earlier stages of steatosis and fibrosis. There is also the additional concern of radiation exposure to the patient.<sup>9</sup> Serological markers are available to assess inflammation and fibrosis developed in NAFLD without radiation exposure. However, these markers are not sensitive to stage hepatic steatosis.<sup>10</sup>

The current preferred imaging modality in the diagnosis of NAFLD is magnetic resonance imaging-based proton density fat fraction (MRI-PDFF). This technique is done by utilizing the multi-echo Dixon method, which discriminates between water and fat proton using the chemical inclusion and exclusion method.<sup>11</sup> Furthermore, MRI-PDFF has been proven to be more sensitive than histology-determined steatosis grading in quantifying fat content in the liver.<sup>12</sup> As such, MRI-PDFF has become a leading non-invasive imaging technique in managing NAFLD.<sup>13</sup> However, the limitations of MRI include high cost, contraindications (claustrophobia), and limited test access in rural areas.

Ultrasonography remains the most commonly used imaging modality to assess hepatic steatosis. This can be attributed to its high diagnostic utility, low cost, ability to be performed at bedside, wide availability, and overall patient tolerability.<sup>14</sup> However, underestimation of hepatic steatosis in individuals with <20% liver adiposity using conventional B-mode ultrasound criteria was reported.<sup>15</sup>

More recently, innovations in quantitative ultrasound biomarkers including two-dimensional attenuation imaging (ATI) have been made that allow for assessing hepatic steatosis with a widely available, cost-efficient, radiation free, and robust technique. ATI assesses the degree of ultrasound energy loss in a localized region of interest (ROI) on B-mode imaging. As reported, ultrasound attenuation coefficients (AC, dB/cm/MHz) assessed by ATI was closely correlated to MRI-PDFF in quantifying hepatic steatosis and intra- and inter-operator reliability in performing ATI was good.<sup>16,17</sup> Yet, the diagnostic scanning protocol of ATI in screening for NAFLD has not been standardized, and technical considerations in performing ATI need to be addressed.

We aimed to assess the variation in the value and diagnostic performance of AC measured at different depths using MRI-PDFF as the reference standard and elaborate on sources of errors in performing liver ATI to screen for NAFLD.

## Materials and methods

The study was conducted through remeasuring AC values on pre-recorded ATI images in 117 adult participants who met inclusion criteria for screening for suspected NAFLD (age >18years old; suspicious or known NAFLD; alcohol intake <20g/day; no history of autoimmune, viral, drug, radiation, or metastasis related liver diseases, tolerant ultrasound and MRI scans) and underwent the ultrasound and MRI scans within 30 days each other in a previous pilot study. The initial study received ethical approval from the Institutional Review Board of Rocky Vista University (IRB#2019-0009) and was performed in accordance with the Declaration of Helsinki (as revised in 2013). All participants provided written informed consent upon enrollment. Additionally, the manuscript was prepared in accordance with Standards for Reporting of Diagnostic Accuracy Studies (STARD) study reporting guidelines. Initially, five liver ATI images were acquired for each participant using a commercial ultrasound scanner equipped with a curvilinear transducer (PVI-475BX, 1.8–6.2 MHz, Aplio i800, Canon Medical Systems USA, Tustin, CA, USA) after fasting 6–8 hours. Liver ACs were measured approximately 2.0 cm below the liver capsule. All ATI images were stored on the hard drive of the scanner. A senior operator with more than 30 years of experience in abdomi-

nal ultrasound and 4 years of experience in ATI performed all initial scans using manufacturer recommended machine settings and scanning protocol.<sup>17</sup> The liver MRI-PDFF were initially performed using a multipoint Dixon technique (Iterative decomposition of water and fat with echo asymmetry and least squares estimation (IDEAL) Intelligent Quotient (IQ), General Electric Healthcare (GE) Healthcare). The methods of MRI-PDFF acquisition used in the initial study included: noncontrast; breath-hold sequence; 3D complex gradient echo; low flip angle; 6 echo-imaging for T2\* decay correction. The average of 9 MRI-PDFF values of the liver was used for analysis.<sup>18</sup> Hepatic steatosis was graded S0 or ≥S1 based on MRI-PDFF value <5% or ≥5%.<sup>13</sup> All liver images were interpreted by three radiologists who had more than 8 years of experience of clinical abdominal/liver imaging in the initial study.

## Ultrasound attenuation imaging

Re-measurements of the liver AC were performed by two junior operators (C.A. and J.D.) who had training in abdominal ultrasound (2 years) and received instruction on how to measure attenuation coefficient of the liver. These two junior operators were blinded to the initial study results of liver AC, MRI-PDFF, and clinical information of the participants. Using the image review function on the ultrasound scanner (Aplio i800, Canon Medical Systems USA), each of 5 ATI images recorded for each liver in the initial scans was selected and displayed on the screen (one on one). The initial AC value and measurement ROI were automatically deleted once the AC measurement function was activated. As a result, a new AC value can be measured by manually placing a region of interest (ROI) in color-coded ATI image. The site of ROI placement for measuring liver AC was confirmed by both operators. The protocol for re-measuring AC of the liver with variable size at different depths was standardized: using depth scales on the ultrasound image as a guidance, the operator manually placed a trapezoid ROI (3.0 cm tall by 3.0 cm wide) in the liver at the depth of 4.5 cm (the distance from the skin to the center of ROI, Fig. 1a), 6 cm (Fig. 1b), 7.5 cm (Fig. 1c), and a large ROI (6.5 cm tall, upper border wide 4 cm, and lower border wide 7.3 cm) that encompassed the entire color-coded region on the ATI image (Fig. 1d). Five ATI images per participant were reviewed. The average of 5 AC values at each depth in the liver were used for analysis. The quality of each AC measurement was evaluated by the R<sup>2</sup> (coefficient of determination) value showed on the screen (Fig. 1a). AC measurements with R<sup>2</sup> < 0.90 were categorized as measurement failure. All measurements were then logged in a Microsoft Excel spread sheet for analysis.

## Statistical Analysis

The Shapiro–Wilk test was used to test the normal distribution of quantitative variables. When quantitative variables were normally distributed, all variables including the distance from the skin to the liver capsule, body mass index (BMI), age of the participants, AC value measured at different ROI depth and size were expressed as mean and standard deviation (SD). Differences in age, BMI, and the distance from the skin to the liver capsule were examined using two-tailed *t*-test. The difference in mean AC value measured at variable ROI depth and size was tested using one-way analysis of variance (ANOVA). The diagnostic performance of AC measured at the different depths were examined using receiver operating characteristic (ROC) curve and displayed with area under ROC (AUC). The area difference under the ROC curves was compared using two-tailed paired-sample Z-test. The measurement failure rate (%) = (number of measurements with R<sup>2</sup> < 0.90 / total number of measurements) at each ROI depth was also calculated. A *p* value less than 0.05 was

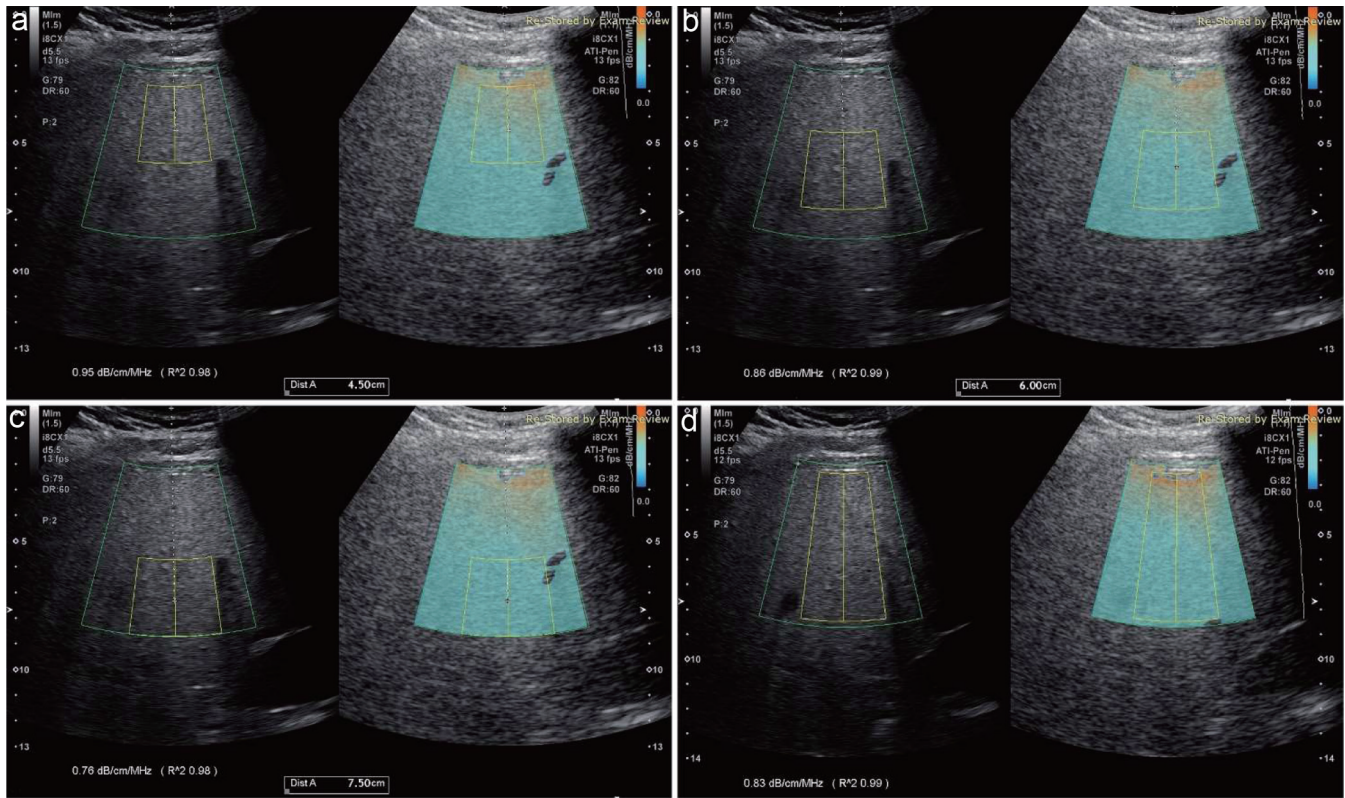


**Fig. 1.** Ultrasound attenuation coefficient (AC, dB/cm/MHz) is measured using two sizes of the region of interest (ROI). A ROI (3 cm tall × 3 cm wide) is placed at the depths of 4.5 cm (the distance from the skin to the center of ROI (a), 6 cm (b), and 7.5 cm (c) in the liver. A larger ROI (d), 6.5 cm tall, 4 cm top border, and 7.3 cm of bottom border) is also used to measure AC of the liver. The AC value is 1.06 dB/cm/MHz, 0.86 dB/cm/MHz, 0.66 dB/cm/MHz, and 0.85 dB/cm/MHz measured at the depths of 4.5 cm, 6 cm, 7.5 cm, and with a large ROI, respectively. AC, attenuation coefficient; ROI, region of interest.

considered statistically significant. Statistical analysis was conducted using the commercial software SPSS (Version 28.0, IBM).

**Results**

Total of 585 AC values (5 AC measurements for each liver) at each ROI depth were measured from 117 participants (49 men and 68 women, mean age 55 years, age range 20–81 years). Based on

MRI-PDFF, 117 participants were divided to normal liver (MRI-PDFF < 5%, n = 27) group or steatotic liver (MRI-PDFF ≥ 5%, n = 90) group (Table 1) (Fig. 2). The difference in the age between the two groups was significant. Differences in BMI or the distance between the skin and the liver capsule between the two groups were not significant (*p* > 0.05, Table 1).

AC measured 0.88 ± 0.21 dB/cm/MHz, 0.73 ± 0.13 dB/cm/MHz, 0.57 ± 0.13 dB/cm/MHz, and 0.72 ± 0.13 dB/cm/MHz at

**Table 1.** Demographic information and AC values in 117 participants with and without NAFLD

Parameter	Normal liver	NAFLD	<i>p</i> *
Participants (M/F)	27 (13/14)	90 (36/54)	
Age (Y)	60 ± 21	51 ± 13	0.04
Body mass index (kg/cm <sup>2</sup> )	30.02 ± 7.51	32.34 ± 5.43	0.28
Distance from the skin to liver capsule (cm)	3.91 ± 0.55	4.08 ± 0.53	0.46
MRI-PDFF (%)	3.38 ± 0.96	14.55 ± 6.73	<0.001
AC measured with large ROI	0.66 ± 0.12	0.74 ± 0.22	<0.01
AC measured at 4.5 cm (dB/cm/MHz)	0.79 ± 0.24	0.92 ± 0.21	<0.01
AC measured at 6 cm (dB/cm/MHz)	0.63 ± 0.10	0.75 ± 0.12	<0.001
AC measured at 7.5 cm (dB/cm/MHz)	0.52 ± 0.13	0.57 ± 0.15	0.10

\**P* is based on two-tailed *t*-test. AC, attenuation coefficient (dB/cm/MHz); MRI-PDFF, magnetic resonance imaging-based proton density fat fraction (%); NAFLD, nonalcoholic fatty liver disease based on MRI-PDFF ≥ 5%.

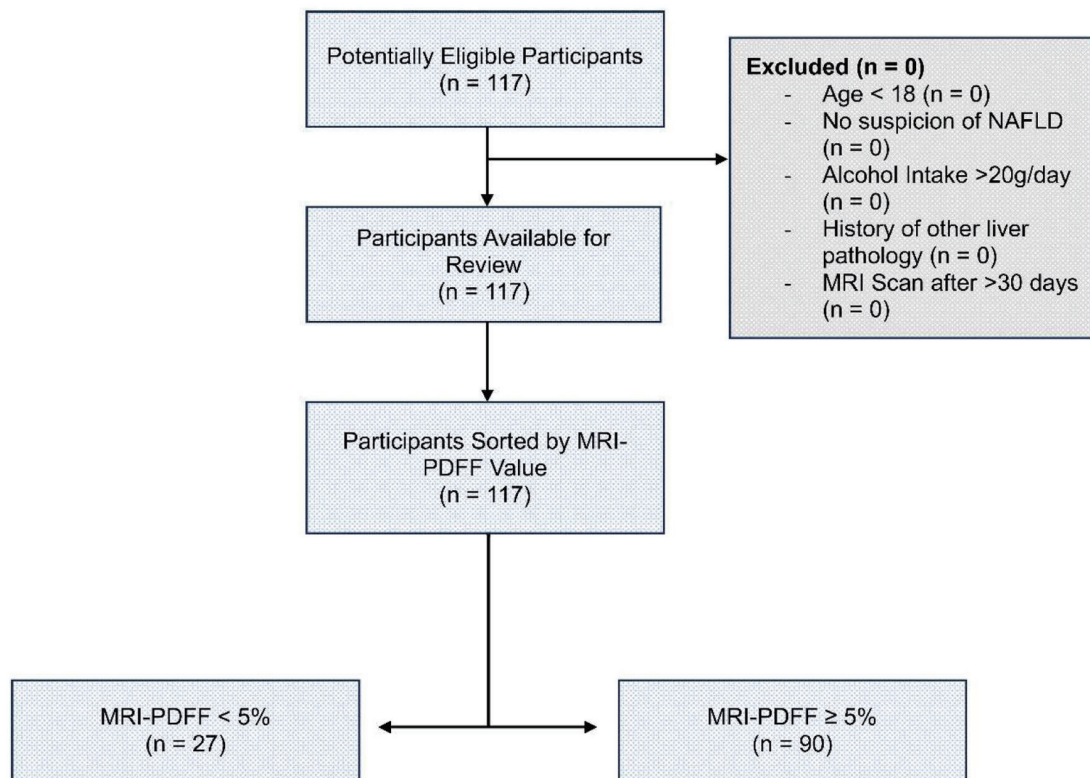


**Fig. 2. Flow and organization of participants through our study.** MRI-PDFF, magnetic resonance imaging-based proton density fat fraction; NAFLD, nonalcoholic fatty liver disease.

ROI depth of 4.5 cm, 6.0 cm, 7.5 cm from the skin and with the large ROI, respectively (Table 2). The difference in AC value measured at variable ROI depth and with different ROI size was significant ( $p < 0.001$ ). The ATI quality represented by  $R^2$  for AC estimation at different depths was listed in Table 2.

The diagnostic performance of AC measured at the different depths was listed in Table 2 and displayed in Figure 3. AC measured at 6 cm showed the highest AUC (AUC = 0.92). There is a

significant difference in the area under ROC curves between AC value measured at 6 cm and those values measured at 4.5 cm, 7.5 cm, and large ROI ( $p < 0.01$ , Table 3). Common sources of pitfalls in performing ATI are discussed in Figure 4.

**Discussion**

We have observed significant differences in liver AC value, as well

**Table 2. Analysis of AC measured at variable depth in screening for NAFLD**

Parameter	ROI at 4.5 cm	ROI at 6 cm	ROI at 7.5 cm	Large ROI	ANOVA (p)
AC (dB/cm/MHz)	0.88 ± 0.21	0.73 ± 0.13	0.57 ± 0.13	0.72 ± 0.13	<0.001
ATI quality (R <sup>2</sup> )	0.88 ± 0.09	0.95 ± 0.06	0.85 ± 0.11	0.91 ± 0.06	<0.001
Failure rate (%)	13/585* (2.2%)	3/585 (0.5%)	68/585 (12%)	7/585 (1.2%)	
ROC (S0 vs ≥ S1)					
Area under ROC (95% CI)	0.720 (0.593–0.847)	0.918 (0.854–0.982)	0.611 (0.501–0.721)	0.683 (0.563–0.803)	
Cutoff value	0.85	0.68	0.60	0.60	
Sensitivity	0.66	0.92	0.57	0.90	
Specificity	0.78	0.82	0.93	0.41	

AC, attenuation coefficient; ANOVA, one-way analysis of variance; ATI, attenuation imaging; CI, Confidence Interval; NAFLD, nonalcoholic fatty liver disease; ROI, region of interest; ROC, Receiver Operating Characteristic. failure rate (%) = (number of cases with  $R^2 < 0.90$  / total number of measurement at each depth); Area under ROC (95% CI), area under the receiver operating characteristic curve (95% confidence interval); cutoff value is based on the maximum Kolmogorov-Smirnov (K-S) statistics and the largest one is reported; ROC (S0 vs ≥ S1), ROC of attenuation coefficient (AC) for determining ≥ mild hepatic steatosis; S0, MRI-PDFF < 5%; ≥S1, MRI-PDFF ≥ 5%; 585\* values = 5 AC measurements/at each depth/per case × 117 cases.

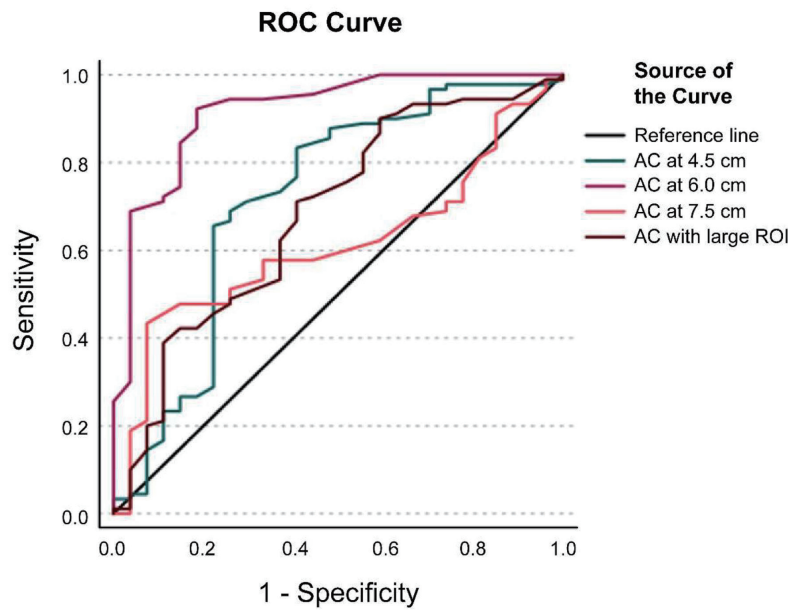


**Fig. 3.** The diagnostic performance of liver attenuation coefficient (AC, dB/cm/MHz) measured at different depths and sizes of the region of interest is analyzed using the area under receiver operating characteristic curve (AUC). AUC of AC measured at the depth of 4.5 cm (green curve), 6.0 cm (purple curve), 7.5 cm from the skin (orange curve), and with the large ROI (brown curve) in determining mild hepatic steatosis ( $\geq S1$ , MRI-PDFF  $\geq 5\%$ ) is 0.72, 0.92, 0.61, and 0.68, respectively. MRI-PDFF, magnetic resonance imaging-based proton density fat fraction; ROC, receiver operating characteristic; ROI, region of interest.

as in ATI quality, and diagnostic performance (AUC) for determining NAFLD among those measured at variable ROI depth and size. Importantly, re-measuring the AC value of the liver on the pre-recorded ATI images stored in the ultrasound scanner hard drive is an ideal method that allows radiologists to remeasure AC in different ROI location and correct technical errors in the AC measurement. As such, the accuracy of interpreting ATI images to assess hepatic steatosis can be improved without a requirement of re-scanning (callback) the patient.

In the study, the best ROI depth for measuring liver AC is at 6 cm from the skin (Fig. 1b) resulting in the highest diagnostic performance of AC to determine  $\geq$  mild hepatic steatosis, ATI quality, and lowest failure rate compared with AC values measured at depths of 4.5 cm, 7.5 cm, and large ROI. The ROI depth at 4.5 cm seemed to be too close to the liver capsule to avoid the dark orange color area produced by high noise or reverberation artifact (Fig.

4a, b) in some patients. The ROI depth at 7.5 cm was often too deep from the skin to exclude the dark blue area (weak echo signal, Fig. 4c) due to less sound penetration,<sup>19</sup> which yielded the poor ATI quality, low diagnostic performance, and high failure rate. The utilization of a large ROI is able to assess tissue attenuation in relative larger region of liver parenchyma (6.5 cm  $\times$  7.3 cm vs. 3 cm  $\times$  3 cm). However, using a large ROI to measure liver AC magnifies technical challenges to place such a large ROI in a small liver (such as a cirrhotic liver) and avoid prominent hepatic vessels (e.g. dilatation of the hepatic veins in congestive heart failure or portal vein in significant portal hypertension). Further, AC measured at the depth of 7.5 failed to distinguish steatotic livers from normal livers as the difference in AC value between normal and steatotic livers was not significant ( $p = 0.10$ , Table 1).

Ultrasound attenuation-based fat quantification technique relies on the assessment of the energy loss of the acoustic signals while

**Table 3.** Comparison the AUC of AC in determining hepatic steatosis

Test result pair(s)	Paired-sample area difference under the ROC curves					
	Asymptotic		AUC difference	Std. error difference <sup>b</sup>	95% Confidence interval	
	z	Sig. (2-tail) <sup>a</sup>			Lower bound	Upper bound
4.5 cm: 6 cm	-3.622	0.000	-0.198	0.309	-0.305	-0.091
4.5 cm: 7.5 cm	1.715	0.086	0.109	0.343	-0.016	0.233
4.5 cm: large ROI	1.125	0.261	0.037	0.345	-0.027	0.101
6 cm: 7.5 cm	5.202	0.000	0.307	0.296	0.191	0.423
6 cm: large ROI	4.479	0.000	0.235	0.303	0.132	0.338
7.5 cm: large ROI	-1.586	0.113	-0.072	0.335	-0.161	0.017

AC, attenuation coefficient; AUC, area under receiver operating characteristic curve; ROI, region of interest. AUC comparison\* is to test the area difference under the ROC curves using a two-tailed paired-sample Z-test; Sig, significance ( $p$  value); 4.5 cm, 6 cm, and 7.5 cm, the distance from the skin to the center of the region of interest for measuring liver attenuation coefficient (AC). Large ROI, the size of region of interest (6.5 cm  $\times$  7.3 cm) for measuring liver AC.

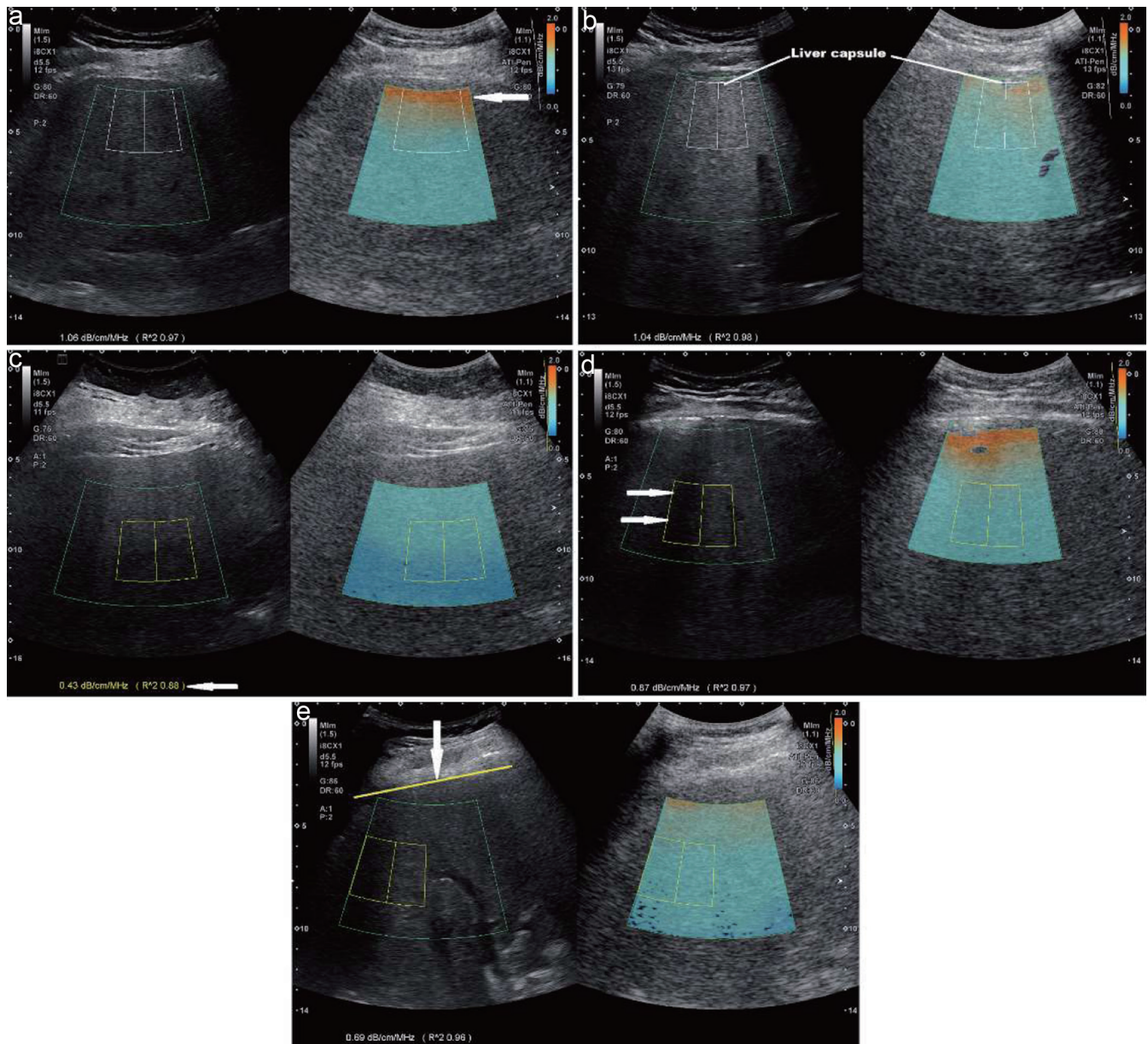


**Fig. 4. Technical errors in measuring liver attenuation coefficient (AC).** Common technical errors in performing liver ultrasound attenuation imaging (ATI) are dark orange area (white arrow, a), the liver capsule (b), the region with blank color at the depth of >10 cm (c, the white arrow points  $R^2 < 0.90$ ), and acoustic shadowing (white arrows, d) included in the measurement ROI. In addition, placing measurement ROI out of the center of the ultrasound attenuation imaging (ATI) image and/or sound beam (white arrow) to liver capsule (yellow solid line) off 90 degrees (e) may also maximize scattering sound energy to various directions resulting in measurement errors.

travelling through the tissue.<sup>20</sup> The distance the sound beam travels, the scanning frequency, and the property of the tissue evaluated effect the ultrasound signal that returns to the transducer.<sup>16,20</sup> As reported, an AC value reflects the degree of acoustic attenuation produced by fat content in the liver and the liver AC estimation is depth dependent.<sup>21</sup> Therefore, it is important to place the ROI at a standardized depth to minimize intra- and inter-observer variation in performing ATI and technical errors among follow up scans for monitoring hepatic steatosis.

Best practices for ATI (Canon Medical Systems) measurement and reporting are still evolving. Besides manufacturer’s recom-

mendation, there is no standardized consensus available to guide performing ATI of the liver.<sup>20</sup> It is important to standardize pre-scan preparation (fasting 6–8 hours), machine settings (scanning frequency), scanning protocols (breath-holding maneuver, intercostal approach), and operator training for performing liver ATI. Further, some technical considerations should be taken when attempting to optimize the efficacy and utility of ATI in the diagnosis and monitoring of hepatic steatosis. There are sources of errors and pitfalls in performing ATI of the liver noted in the study.

1. The region below the liver capsule appearing dark orange color on ATI is produced by ultrasound reverberation artifact

- (Fig. 4a). Therefore, dark-orange color below the liver capsule should be excluded from ROI for measuring liver AC.<sup>22</sup>
- The liver capsule should be excluded from the measurement ROI (Fig. 4b).
  - The posterior region with dark blue (Fig. 4c) or blank color should be avoided from measurement ROI.<sup>23</sup>
  - Acoustic shadowing behind the ribs and/or lung (Fig. 4d) should be avoided from the measurement ROI.
  - The propagation direction of the ultrasound beam is not perpendicular to the liver capsule. Angling of the liver capsule (Fig. 4e) may cause stronger sound beam reflection and refraction once the angle between sound beam and the liver capsule is off 90 degrees,<sup>16</sup> which may affect AC estimation.

This study has several limitations. First, liver biopsy was not available as the reference to assess the accuracy of AC in quantifying hepatic steatosis. We employed MRI-PDFF as the reference standard, which has been used as an acceptable non-invasive alternative measure for quantifying fat content in the liver.<sup>16,24</sup> Second, only one senior operator (J.G.) performed all the ultrasound scans and interobserver variability was not tested in this study, however, good to excellent reproducibility was demonstrated in a training session prior to the study.<sup>17</sup> Third, our study included a large number of participants with obesity (54% participants with BMI > 30 kg/cm<sup>2</sup>; 90% participants with BMI >25 kg/cm<sup>2</sup>). Obesity can significantly alter the placement of ROI within the liver parenchyma due to varying amounts of subcutaneous adipose tissue. Therefore, the recommended placement of ROI at a depth of 6 cm from skin surface may be suitable for patients with BMI ≥ 30 based on our results. However, the ROI placement for estimating liver AC should be adjusted according to the level of comorbid obesity and the thickness of the subcutaneous adipose tissue. As such, measurement failure rate at the measurement depth of 7.5 cm was higher than at depths of 4.5 cm and 6.0 cm. Additionally, the placement of ROI for estimating liver AC should be adjusted according to varying levels of subcutaneous adipose tissue, especially in thin patients with NAFLD. Fourth, we did not analyze confounding factors, such as liver inflammation and fibrosis that may affect liver AC measurement because of the lack of biopsy pathology as a reference. Fifth, we only measured liver AC at the depths of 4.5 cm, 6.0 cm, and 7.5 cm. However, AC measured at the other depths (such as 6.5 cm, 7.0 cm) may be more appropriate than the introduced protocol for individual participant based on his/her body habitus. Sixth, the sample size of the study was small and patient population utilized in this study demonstrated a significant difference in age of participants between the NAFLD and normal liver groups. A low inverse correlation between the age and liver MRI-PDFF was observed (Pearson correlation  $r = -0.18$ ,  $p = 0.08$ ), which is consistent with a previously reported inverse correlation between the age and patients with NAFLD in the general population.<sup>25</sup> Thus, an age matched study in populations with and without NAFLD is warranted. Lastly, the ultrasound scanner hardware and software used in the study were designed by a single ultrasound vendor. The variation in measuring liver attenuation coefficient by using ultrasound scanners and software designed by different vendors needs further investigation. Clinical and biomedical engineering researchers at the American Institute of Ultrasound in Medicine (AIUM)-RSNA Quantitative Imaging Biomarkers Alliance (QIBA) Pulse-Echo Quantitative Ultrasound (PEQUS) initiative for fat quantification are working on standardization of ultrasound attenuation coefficient technique for clinical application.<sup>20</sup> NAFLD is a common disorder affecting liver and cardiovascular systems. Following the validation of multiple quantitative imaging including ultrasound

and MRI biomarkers to assess hepatic steatosis, the development and implementation of artificial intelligence and machine learning models in performing ultrasound attenuation imaging in NAFLD management is encouraged.

In conclusion, the ROI depth significantly influences the diagnostic performance and value of liver AC estimation. The best ROI location to measure liver AC in patients with BMI ≥ 30 may be at a depth of 6 cm from the skin. Technical considerations should be taken in performing ATI for assessing hepatic steatosis in patients with variable thickness of the subcutaneous tissue. Excluding reverberation, the region with blank color, and acoustic shadowing from measurement ROI, and AC value with  $R^2 < 0.90$  should be taken into consideration when scanning and interpreting ATI to screen for NAFLD. The study results provide the reference to develop a standardized protocol in performing ATI.

### Acknowledgments

Authors thank Canon Medical Systems USA for providing grant and equipment to support the study.

### Funding

Jing Gao received research fund and loaned ultrasound equipment from Canon Medical Systems USA.

### Conflict of interest

All other authors have no conflict of interests related to this publication.

### Author contributions

Study concept and design (JG), acquisition of data (CA, JD, JG), analysis and interpretation of data (JG, ML), drafting of the manuscript (CA, JD), critical revision of the manuscript for important intellectual content (JG, JJ, LDH, ML), technical, or material support (LDH, JJ), and study supervision (JG). All authors have made a significant contribution to this study and have approved the final manuscript.

### Ethical statement

The initial study received ethical approval from the Institutional Review Board of Rocky Vista University (IRB#2019-0009) and was performed in accordance with the Declaration of Helsinki (as revised in 2013). All participants provided written informed consent upon enrollment.

### Data sharing statement

Study data are available from the corresponding author upon reasonable requests.

### References

- Perumpail BJ, Khan MA, Yoo ER, Cholankeril G, Kim D, Ahmed A. Clinical epidemiology and disease burden of nonalcoholic fatty liver disease. *World J Gastroenterol* 2017;23(47):8263–8276. doi:10.3748/wjg.v23.i47.8263, PMID:29307986.
- Chalasan N, Younossi Z, Lavine JE, Charlton M, Cusi K, Rinella M, et

- al*. The diagnosis and management of nonalcoholic fatty liver disease: Practice guidance from the American Association for the Study of Liver Diseases. *Hepatology* 2018;67(1):328–357. doi:10.1002/hep.29367, PMID:28714183.
- [3] Byrne CD, Targher G. NAFLD: a multisystem disease. *J Hepatol* 2015;62:S47–S64. doi:10.1016/j.jhep.2014.12.012, PMID:25920090.
- [4] Marchesini G, Brizi M, Bianchi G, Tomassetti S, Bugianesi E, Lenzi M, *et al*. Nonalcoholic fatty liver disease: a feature of the metabolic syndrome. *Diabetes* 2001;50(8):1844–1850. doi:10.2337/diabetes.50.8.1844, PMID:11473047.
- [5] Adams LA, Angulo P, Lindor KD. Nonalcoholic fatty liver disease. *CMAJ* 2005;172(7):899–905. doi:10.1503/cmaj.045232, PMID:15795412.
- [6] Rinella ME, Sanyal AJ. Management of NAFLD: a stage-based approach. *Nat Rev Gastroenterol Hepatol* 2016;13(4):196–205. doi:10.1038/nrgastro.2016.3, PMID:26907882.
- [7] Li Q, Dhyani M, Grajo JR, Sirlin C, Samir AE. Current status of imaging in nonalcoholic fatty liver disease. *World J Hepatol* 2018;10(8):530–542. doi:10.4254/wjh.v10.i8.530, PMID:30190781.
- [8] Salva-Pastor N, Chávez-Tapia NC, Uribe M, Nuño-Lámbarrri N. The diagnostic and initial approach of the patient with non-alcoholic fatty liver disease: role of the primary care provider. *Gastroenterol Hepatol Bed Bench* 2019;12(4):267–277. PMID:31749914.
- [9] Lee SS, Park SH, Kim HJ, Kim SY, Kim MY, Kim DY, *et al*. Non-invasive assessment of hepatic steatosis: prospective comparison of the accuracy of imaging examinations. *J Hepatol* 2010;52(4):579–585. doi:10.1016/j.jhep.2010.01.008, PMID:20185194.
- [10] Dumitrascu DL, Neuman MG. Non-alcoholic fatty liver disease: an update on diagnosis. *Clujul Med* 2018;91(2):147–150. doi:10.15386/cjmed-993, PMID:29785151.
- [11] Reeder SB, Cruite I, Hamilton G, Sirlin CB. Quantitative Assessment of Liver Fat with Magnetic Resonance Imaging and Spectroscopy. *J Magn Reson Imaging* 2011;34(4):729–749. doi:10.1002/jmri.22775, PMID:22025886.
- [12] Noureddin M, Lam J, Peterson MR, Middleton M, Hamilton G, Le TA, *et al*. Utility of magnetic resonance imaging versus histology for quantifying changes in liver fat in nonalcoholic fatty liver disease trials. *Hepatology* 2013;58(6):1930–1940. doi:10.1002/hep.26455, PMID:23696515.
- [13] Middleton MS, Heba ER, Hooker CA, Bashir MR, Fowler KJ, Sandrasegaran K, *et al*. Agreement Between Magnetic Resonance Imaging Proton Density Fat Fraction Measurements and Pathologist-Assigned Steatosis Grades of Liver Biopsies From Adults With Nonalcoholic Steatohepatitis. *Gastroenterology* 2017;153(3):753–761. doi:10.1053/j.gastro.2017.06.005, PMID:28624576.
- [14] Mishra P, Younossi ZM. Abdominal ultrasound for diagnosis of nonalcoholic fatty liver disease (NAFLD). *Am J Gastroenterol* 2007;102(12):2716–2717. doi:10.1111/j.1572-0241.2007.01520.x, PMID:18042105.
- [15] Dasarathy S, Dasarathy J, Khiyami A, Joseph R, Lopez R, McCullough AJ. Validity of real time ultrasound in the diagnosis of hepatic steatosis: a prospective study. *J Hepatol* 2009;51(6):1061–1067. doi:10.1016/j.jhep.2009.09.001, PMID:19846234.
- [16] Jeon SK, Lee JM, Joo I, Yoon JH, Lee DH, Lee JY, *et al*. Prospective Evaluation of Hepatic Steatosis Using Ultrasound Attenuation Imaging in Patients with Chronic Liver Disease with Magnetic Resonance Imaging Proton Density Fat Fraction as the Reference Standard. *Ultrasound Med Biol* 2019;45(6):1407–1416. doi:10.1016/j.ultrasmedbio.2019.02.008, PMID:30975533.
- [17] Gao J, Lee R, Trujillo M. Reliability of Performing Multiparametric Ultrasound in Adult Livers. *J Ultrasound Med* 2022;41(3):699–711. doi:10.1002/jum.15751, PMID:33982805.
- [18] Gao J. Ultrasound attenuation coefficient of the liver and spleen in adults: A preliminary observation. *Clin Imaging* 2022;84:140–148. doi:10.1016/j.clinimag.2022.02.010, PMID:35217283.
- [19] Ferraioli G, Berzigotti A, Barr RG, Choi BI, Cui XW, Dong Y, *et al*. Quantification of Liver Fat Content with Ultrasound: A WFUMB Position Paper. *Ultrasound Med Biol* 2021;47(10):2803–2820. doi:10.1016/j.ultrasmedbio.2021.06.002, PMID:34284932.
- [20] Ferraioli G, Kumar V, Ozturk A, Nam K, de Korte CL, Barr RG. US Attenuation for Liver Fat Quantification: An AIUM-RSNA QIBA Pulse-Echo Quantitative Ultrasound Initiative. *Radiology* 2022;302(3):495–506. doi:10.1148/radiol.210736, PMID:35076304.
- [21] Bae JS, Lee DH, Lee JY, Kim H, Yu SJ, Lee JH, *et al*. Assessment of hepatic steatosis by using attenuation imaging: a quantitative, easy-to-perform ultrasound technique. *Eur Radiol* 2019;29(12):6499–6507. doi:10.1007/s00330-019-06272-y, PMID:31175413.
- [22] Ferraioli G, Maiocchi L, Raciti MV, Tinelli C, De Silvestri A, Nichetti M, *et al*. Detection of Liver Steatosis With a Novel Ultrasound-Based Technique: A Pilot Study Using MRI-Derived Proton Density Fat Fraction as the Gold Standard. *Clin Transl Gastroenterol* 2019;10(10):e00081. doi:10.14309/ctg.0000000000000081, PMID:31609745.
- [23] Ferraioli G, Maiocchi L, Savietto G, Tinelli C, Nichetti M, Rondanelli M, *et al*. Performance of the Attenuation Imaging Technology in the Detection of Liver Steatosis. *J Ultrasound Med* 2021;40(7):1325–1332. doi:10.1002/jum.15512, PMID:32960457.
- [24] Cassidy FH, Yokoo T, Aganovic L, Hanna RF, Bydder M, Middleton MS, *et al*. Fatty liver disease: MR imaging techniques for the detection and quantification of liver steatosis. *Radiographics* 2009;29(1):231–260. doi:10.1148/rg.291075123, PMID:19168847.
- [25] Lin Y, Feng X, Cao X, Miao R, Sun Y, Li R, *et al*. Age patterns of non-alcoholic fatty liver disease incidence: heterogeneous associations with metabolic changes. *Diabetol Metab Syndr* 2022;14(1):181. doi:10.1186/s13098-022-00930-w, PMID:36443867.